American Mineralogist, Volume 81, pages 395–403, 1996

Channel occupancy in an alkali-poor beryl from Serra Branca (Goias, Brazil): Spectroscopic characterization

BERNARD CHAROY,[1] PHILIPPE DE DONATO,[2] ODILE BARRES,[2] AND CRISTINA PINTO-COELHO[3,*]

[1]ENSGéologie de Nancy-CRPG (CNRS), B.P. 20, 54501 Vandoeuvre-les-Nancy Cedex, France
[2]ENSGéologie de Nancy, LEM-URA 235 (CNRS), B.P. 40, 54501 Vandoeuvre-les-Nancy Cedex, France
[3]CNPq, Department of Earth Sciences, Universidade de Brasília, Brasília, Brazil

ABSTRACT

Spectroscopic (micro FTIR, Raman, MAS NMR) and mass spectroscopic techniques have been used to examine, on both single-crystal and powder samples, the behavior of H_2O and CO_2 molecules in the structural channels of an alkali-poor, volatile-rich beryl from Brazil. Polarized single-crystal FTIR and Raman spectra were obtained on oriented wafers of isolated crystals. Location and orientation of H_2O and CO_2 molecules were determined from IR spectra. The proton-proton vectors of type-I and type-II H_2O are parallel and perpendicular to the *c* axis, respectively; the molecular axis of the CO_2 molecule is perpendicular to the *c* axis. Relative proportions of both types of H_2O were determined from their respective IR absorption-band intensities and were found to be nearly equivalent. There is, contrary to what is generally claimed in the literature, no relation between alkali and type-II H_2O contents. Absorptivity coefficients for H_2O and CO_2 were computed for every specific orientation. A ^1H MAS NMR spectrum resolved as a "Pake" doublet seems to confirm the absence of any anisotropic movement of the H_2O molecules from one orientation to the other on the NMR time scale. Mass discrimination of volatiles released by pyrolysis under vacuum confirms the weak mobility of H_2O and CO_2 molecules in the channel sites, although the plugging effect of alkalis in the channels can be neglected for such an alkali-poor beryl. The volatile vs. alkali content ratio in beryl could possibly be used as an environmental indicator.

INTRODUCTION

Beryl is an accessory mineral present mainly in pegmatites but also in some highly evolved granites (Charoy and Noronha 1996) and some metamorphic rocks. Beryl is a typical example of the ring silicate class. Its honeycomb structure consists of stacked six-membered rings of Si tetrahedra forming large open channels that parallel the *c* axis. These channels pinch to bottlenecks ~2.8 Å (C2) in diameter or swell to large cages ~5.1 Å (C1) in diameter. Rings are crosslinked by Be tetrahedra and Al octahedra (Gibbs et al. 1968).

Chemical compositions of natural beryl substantially deviate from the ideal formula $Al_2Be_3Si_6O_{18}$ owing to complex cationic substitutions. Alkalis (mainly Na and Cs for charge balance), because they are too large to substitute in fourfold or sixfold coordination within the structure, must be accommodated in the vacant channels. Though beryl is a nominally anhydrous mineral, channels also typically contain isolated H_2O and CO_2 molecules, together with rare gases (He and Ar, Damon and Kulp 1958). Alkalis and free volatile molecules occupy variable positions in the channel (Gibbs et al. 1968; Wood and Nassau 1968; Aurisicchio et al. 1994). H_2O within the structure has been classified as type I or II, depending on the orientation of the twofold axis of symmetry of the molecule relative to the *c* axis of beryl: perpendicular as type I and parallel as type II (the reference work of Wood and Nassau 1968). Because of its size, the linear CO_2 molecule must be normal to the *c* axis and parallel to the larger dimension of the channel. Normal (unsubstituted or weakly substituted) beryl shows the almost exclusive presence of type-I H_2O, whereas type-II H_2O becomes dominant when cationic substitution, in fourfold or sixfold coordination, increases. Therefore, type-II H_2O should be roughly coupled with the incorporation of alkalis into channels (Aurisicchio et al. 1988; Sherriff et al. 1991). Such a relation has been observed in cordierite (Armbruster 1986).

Since the 1960s, there have been numerous infrared and other spectroscopic investigations of the mobility of these volatile molecules (Wickersheim and Buchanan 1959; Boutin et al. 1964; Pedersen 1964, among others). However, results are still controversial, and even recent papers (Sherriff et al. 1991; Artioli et al. 1993) remain ambiguous.

In contrast to cordierite, a very closely related, volatile-

* Present address: CRPG (CNRS), B.P. 20, 54501 Vandoeuvre-les-Nancy Cedex, France.

0003–004X/96/0304–0395$05.00

TABLE 1. Chemical analyses and structural formulas of beryl and phengite

wt%	1 Wet analysis beryl	2 Wet analysis phengite	3 Corrected beryl	4 Microprobe beryl		3 Beryl	4 Beryl
						T″ site	
SiO_2	63.21	46.78	64.97	65.06(0.50)	Si	6.000	6.000
TiO_2	0.01	tr.	—	—		**Octahedral site**	
Al_2O_3	19.54	33.23	17.28	17.05(0.25)	Al	1.888	1.867
Fe_2O_3	0.83	2.62	0.55		Fe^{3+}	0.037	
FeO	0.28	0.86	0.20	1.21(0.05)	Fe^{2+}	0.017	0.095
MnO	0.02	0.05	—	0.02(0.02)	Mn	—	0.002
MgO	0.17	0.25	0.15	0.11(0.02)	Mg	0.017	0.015
CaO	0.14	—	0.14	—	Ca	0.011	0.021
Na_2O	0.47	0.30	0.46	0.60(0.03)	□	0.030	0.021
K_2O	1.42	10.80	0	0.01(0.01)		**T′ site**	
P_2O_5	0.10	0.08	—	n.d.	Be	2.958	2.956
BeO	11.66	—	13.27	n.d.	Si	0.028	0.038
H_2O^+	2.17	3.75	1.91	n.d.	P	0.005	—
H_2O^-	0.17	n.d.	—		□	0.009	0.006
CO_2	0.17	n.d.	0.19	n.d.		**2a site**	
F	0.10	1.38	—	—	Na	0.078	0.108
					K	—	0.001
O = F	0.04	0.58					
					Fe^{3+}/Fe^{2+}	2.18	
Sum	100.42	99.52	99.12	84.06			

Note: Wet chemical analyses of beryl (1) and hosting phengite (2). Corrected analysis of beryl after muscovite subtraction (3). Average of 14 spots on beryl by electron microprobe (4). Trace elements (in parts per million) Li = 66, Rb = 1.48, Cs = 16, and Cr < 10 in the analysis 1. Structural formulas (on the basis of 18 O) for beryl (3 and 4, the same Be content used for both). O atoms of H_2O and CO_2 molecules were not included in the calculation of the structural formula; □ represents vacancy.

rich ring-silicate that was extensively studied as a metamorphic volatile index (Zimmermann 1981; Johannes and Schreyer 1981; Lamb 1985; Vry et al. 1990), beryl was investigated only minimally as a volatile vector and never as an environmental marker for monitoring the composition of the fluids from which it has grown (Staatz et al. 1965; Černý and Turnock 1975). Most of the beryl samples studied in the literature are from granitic pegmatites, and few results on hydrothermal (natural or synthetic) beryl are available. The present study is a spectroscopic investigation of the location, bonding state, and dynamic behavior of protons in a natural, low-temperature and alkali-depleted beryl.

BERYL SAMPLES

Single crystals of beryl were used for this study. They were selected by hand-picking from hydrothermal veins (mostly composed of fine-grained greenish phengite flakes) that crosscut both granites and derivative greisen metasomatites of the Serra Branca Body, Goias, Central Brazil (de Andrade 1978). Beryl occurs as scattered crystals without any structural orientation. Crystals, up to 7 cm long, are euhedral with a characteristic barrel shape. They are greenish yellow and poorly translucent. The length-to-width ratio is independent of the size. In thin section, beryl crystals are systematically crowded by white mica (on average 15% in volume from point counting and image analysis) as scattered minute flakes (from 5 to 10 μm) or as clusters of larger laths (100 μm) identical to those in the host rock. Contacts with the mica-rich host rock are sharp, without any evidence of corrosion (disequilibrium) of the beryl. They are surprisingly devoid of fluid inclusions large enough to be studied by microthermometry.

STRUCTURAL AND CHEMICAL DATA

Beryl from Serra Branca, because of the abundance of unavoidable mica inclusions, was not subjected to single-crystal X-ray analysis, and unit-cell parameters were obtained by the powder method. Twenty-five unequivocally indexed diffraction lines in the 3–32° 2θ range (lines from mica inclusions were avoided) were used to refine the cell dimensions (computation using the Win Metric system of the Siemens software). Systematic absences of the type *hhl* and *h0l* (*l* odd) reflections are consistent with the space group symmetry *P6/mcc* (Gibbs et al. 1968). Cell parameters are as follows: $a = 9.215(3)$, $c = 9.190(7)$ Å, $V = 675.918(10)$ Å^3, c/a ratio = 0.997. Such a ratio is indicative of the unsubstituted, normal beryl type (Aurisicchio et al. 1994).

Beryl samples were analyzed by wet chemistry and by electron microprobe [SX50 Cameca microprobe housed at Nancy I University, PAP correction procedures: Pouchou and Pichoir (1991)]. Beryl appears homogeneous (Table 1) at microprobe detection limits, without any compositional zoning exceeding the statistical uncertainty of the method. Because of the contamination by mica, the wet-chemical analysis represents a composite and must therefore be corrected. Because natural beryl is nearly devoid of K (Bakakin and Belov 1962; de Almeida Sampaio Filho and Sighinolfi 1973; Aurisicchio et al. 1988, among others), the complete analysis was recomputed by removing all K_2O and the associated chemical composition of the mica inclusions (analysis of a mica

separate from the host rock is shown in Table 1). The resultant composition is reported in Table 1. Both compositions (global and in situ) compare well except for Na content, which is higher in the microprobe analysis (Na was analyzed first to avoid any loss during the experiment). Structural formulas (based on 18 O atoms) are also listed in Table 1. The T″ site is filled completely by Si, and ring tetrahedra are uniformly occupied. The deficiency of $^{[6]}$Al is not fully compensated by divalent and trivalent cations, and an octahedral vacancy of 0.030 atoms per formula unit (apfu) is still present. Li is lacking. The Be tetrahedral T′ site is partly filled by Si (0.028 apfu), but some vacancy persists, in part balanced by P. However, Al and Be contents are close to stoichiometric values: 2 and 3 apfu, respectively. Such a crystal composition approaches that of a normal unsubstituted beryl with a composition close to the ideal stoichiometry (Aurisicchio et al. 1988) despite some octahedral substitution. Na (no Cs), which enters the beryl structure to satisfy positive-charge deficiency, is present only in low concentration [low alkali-bearing beryl: group II of Schmetzer (1989)]. The Fe^{3+}/Fe^{2+} ratio of 2.18 is quite high and similar to that presented by the mica from outside (ratio of 2.75). Such a high $X_{Fe^{3+}}$ ratio would indicate fairly oxidizing conditions during the precipitation of the vein material, in accordance with the significant CO_2 content in the beryl channel (see below). H_2O was determined volumetrically by Karl Fischer titration after heating the sample to 1250 °C, and CO_2 by pulse coulometric titration after ignition to 1100 °C. Volatile content (H_2O = 1.91 and CO_2 = 0.18 wt%) is high, which is normal in natural beryl from a source other than pegmatites (only one natural beryl is described as H_2O free in the literature; Aurisicchio et al. 1988).

Spectroscopic data

Several methods were used to investigate location, orientation, and motion of volatile species hosted in the channels of beryl.

Vibrational spectroscopy

The fundamental vibrational modes (symmetric ν_1, ν_2, and asymmetric ν_3) of free molecular H_2O and CO_2 have been extensively described in the literature (see Nakamoto 1963). All vibrations of H_2O and CO_2 molecules, except the ν_1 vibration of CO_2, are IR active. On the other hand, all vibrations of H_2O and the ν_1 vibration of CO_2 are Raman active, but ν_2 and ν_3 vibrations of CO_2 are Raman inactive. However, conflict may result when intensities of overtone and combination bands are close to those of fundamentals (Fermi resonance). This is the case for the first overtones of the ν_2 and ν_1 vibrations of CO_2, which can interact to form two strong Raman lines at 1388 and 1286 cm^{-1} (Nakamoto 1963).

Micro FTIR spectroscopy. Infrared absorption spectra were obtained at room temperature from oriented, doubly polished, 50 μm thick wafers of five crystals of beryl. Crystals were oriented parallel or normal to the c axis,

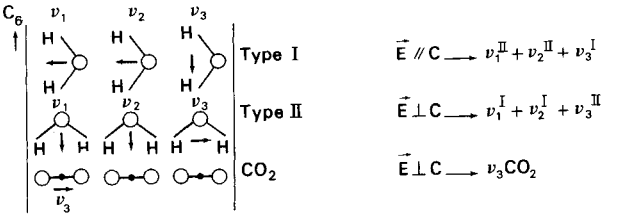

FIGURE 1. Schematic representation of the dipole moment vectors of the fundamental modes of vibration for type-I and type-II H_2O and possible interactions with regard to the orientation of the electric vector, **E**.

using their external morphology and conoscopic interference figures. IR spectra in the frequency range 4000–600 cm^{-1} were recorded with a Bruker IFS 88 Fourier-transform infrared (FTIR) microspectrometer equipped with a Globar source and an MCT detector. The beam size was reduced to 60 μm. Spectral resolution was set at 4 cm^{-1}. The time-averaged signal was collected over 200 scans. Background effects due to atmospheric H_2O and CO_2 were subtracted. Spectra were recorded with a transmitted, unpolarized and polarized IR beam, using a wire-grid Harrick turning polarizer. Three frequency regions are particularly important: 3800–3500 cm^{-1} (H_2O stretching frequency), 2400–2300 cm^{-1} (CO_2 asymmetric stretching frequency), 1700–1500 cm^{-1} (H_2O bending frequency). As shown in Figure 1, the incident beam interacts with $\nu_3^I + \nu_1^{II} + \nu_2^{II}$ when **E** (the electric vector) is parallel to the c axis, and with $\nu_1^I + \nu_2^I + \nu_3^{II}$ when **E** is perpendicular to the c axis (I and II indices refer to type-I and type-II H_2O, respectively). Two selections of spectra obtained from different crystallographic orientations (parallel and perpendicular to the c axis) are shown in Figure 2, with different orientations of the polarized electric vector. The progressive drift in the peak heights and locations (Fig. 2a) demonstrates fairly conclusively the relative orientations of the two types of H_2O molecules in the channel, in accordance with what is predicted in Figure 1. In the bending region, ν_2^I vibration is found at 1605 cm^{-1} (partly residual when **E** is parallel to the c axis). All modes of both types of H_2O except the ν_1^I mode (Table 2) compare fairly well with previous data obtained by Wood and Nassau (1968). In our case, and accounting for the difference $\nu_3^{II} - \nu_1^{II}$ (Δ^{II}_{3-1} = 68 cm^{-1}), the position of ν_1^I is found at 3647 (Δ^I_{3-1} = 47 cm^{-1}) or 3630 (Δ^I_{3-1} = 64 cm^{-1}) cm^{-1}. In general, hydrogen bonds lower the mode frequency and introduce some broadening of the libration bands. The slight energy decrease of 60–100 cm^{-1} for the IR stretching modes compared with those of H_2O vapor [Nakamoto (1963) in Table 2] precludes any strong hydrogen bond with O of the structure, in accordance with the nonenergetic "bottle model" defined by Barton (1986) from thermodynamic considerations. Therefore, H_2O molecules are loosely bonded to the silicate framework and are able to vibrate rather freely into the channels. In addition to the classical types I and II, a supple-

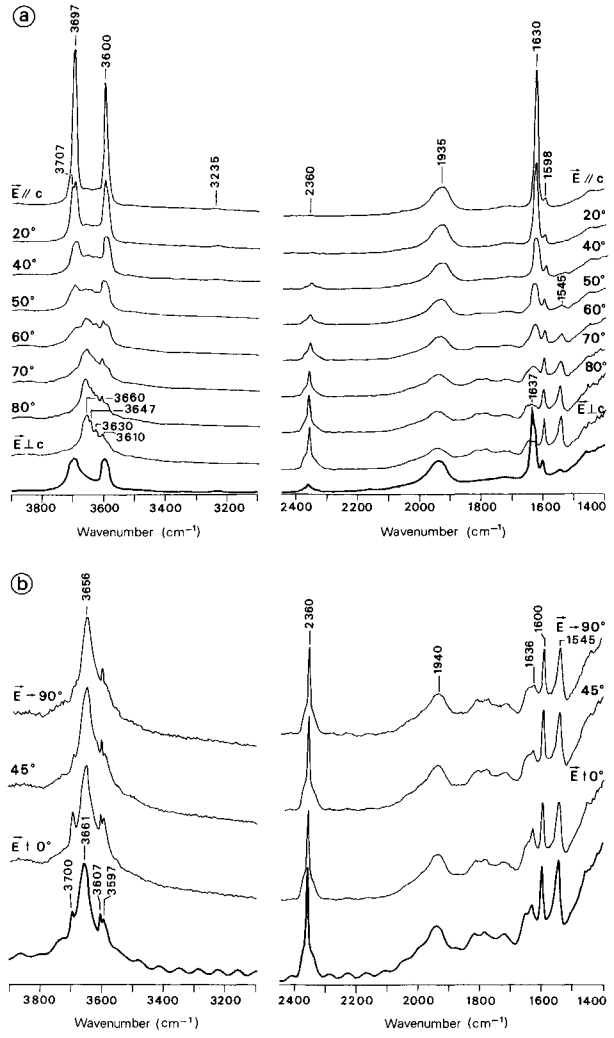

FIGURE 2. Infrared absorption spectra of single crystals of beryl at room temperature with unpolarized (bold line) and polarized radiation: (**a**) section where the *c* axis is horizontal, (**b**) section normal to the *c* axis.

mentary but small H_2O population is discerned around 3235 cm^{-1}, with an orientation parallel to the *c* axis and without any apparent bending counterpart. Such frequency is generally assigned to H_2O with a compact structure of ice (Franks 1972). This band was also present but not explained in the spectra given by Wood and Nassau (1968).

CO_2 presents only one strong band at 2360 cm^{-1} and definitely has a strict orientation with the O-C-O vector perpendicular to the *c* axis (it disappears progressively in Fig. 2a but is unchanged in Fig. 2b). Because the peak intensity of CO_2 is constant in Figure 2b, for any orientation of **E**, it is clear that the molecule is isotropically distributed in the (0001) plane. The base of the peak is slightly enlarged and asymmetrical. The four absorption bands (2283, 2307, 2348, and 2390 cm^{-1}) assigned to

TABLE 2. Principal vibrational bands (major in bold) for type-I and type-II H_2O and CO_2 from in situ and KBr pellet experiments

		This study		Wood and Nassau 1967	Frequency difference
		(cm^{-1}) in situ	(cm^{-1}) KBr pellet	(cm^{-1}) in situ	(cm^{-1}) $\nu_{mol} - \nu_{cry}$
H_2O Type I	$\nu 1$	3610–3630–3647	**3629**	3555	+23
	$\nu 2$	1602–**1550**		1595	+50
	$\nu 3$	**3697**	**3698**	3694	+57
H_2O Type II	$\nu 1$	**3592**	**3597**	3592	+60
	$\nu 2$	1630–**1637**		1628	−40
	$\nu 3$	**3660**	**3654**	3655	+96
CO_2		**2360**	**2361**	2354	−12

Note: Comparison with Wood and Nassau's (1967) data. Difference in vibrational frequencies between in situ experiments and H_2O-CO_2 vapor (Nakamoto 1963).

CO_2 in cordierite by Le Breton (1989) and Visser et al. (1994) were not observed. As a first hypothesis, the band at 1545 cm^{-1} can be assigned to the CO_2 molecule (ν_3) in a pseudocarbonate structure because of its interaction with one O atom of the silica ring.

The omnipresent band near 1950 cm^{-1}, for any polarization orientation, can be related to an overtone absorption of a lattice mode, possibly originating in the hexagonal silicate ring (Wood and Nassau 1968; Aines and Rossman 1984).

As seen above, H_2O and CO_2 are easily resolved in IR spectra. Their respective proportions can be deduced from the absorbance intensities of their ν_3 stretching vibrations (type-I and type-II H_2O and CO_2), assuming that Beer's law can be applied. An IR spectrum in the 4000–2000 cm^{-1} region (Fig. 3) was obtained from two KBr pellets prepared with the experimental conditions (diameter and thickness of the pellet, weight ratio of beryl/KBr) of Vry et al. (1990) for cordierite. Grain size was <2 μm. According to the standard IR literature (Duyckaerts 1959), it has been experimentally verified that the intensity of the IR absorption band remains unchanged for grain sizes of 2 μm or less. Three transmission measurements were made on each pellet with good reproducibility of the intensity and location of the main absorption bands. OH stretching of phengite at 3628 cm^{-1}, from a spectrum obtained in situ from a crystal included in a beryl wafer, does not prevent us from determining peak heights for ν_3 stretching bands. The ν_1 and ν_3 bands of beryl were converted to the respective contents of type-I and type-II H_2O (Table 3). A similar calculation was made using the absorbance values from in situ experiments and the ϵ values (molar absorptivity coefficients in liters per mole-centimeter) listed in Table 3. Coefficients were found to be equal for both types of H_2O but strongly different from those [$\epsilon_{CO_2} = 630$; ϵ_{H_2O} (I or II) = 77] recommended by Vry et al. (1990) for powdered cordierite. The ratios of absorptivity coefficients for CO_2 and H_2O from KBr pellet or in situ experiments are 4.5 and 1.6, respectively, in

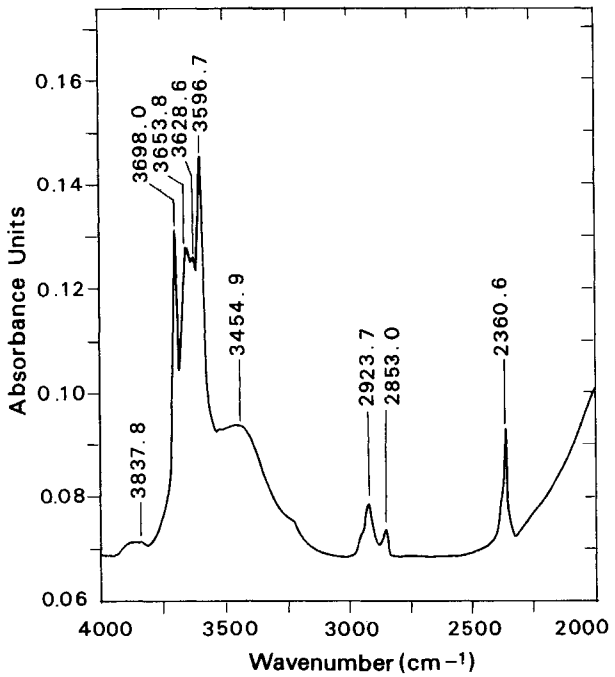

FIGURE 3. Infrared spectrum of powdered beryl in the range of the stretching modes of H_2O and CO_2 (unpolarized radiation). Experimental conditions were the same as those used by Vry et al. 1990: KBr pellets prepared from 3 mg of ground beryl and 100 mg of dry KBr; the pellets were 13 mm in diameter and 0.3 mm thick.

marked contrast to those cited by Goldman et al. (1977) and Aines and Rossman (1984) for cordierite. As demonstrated above, maxima of absorbance were obtained for very restrictive crystal orientation with regard to the incident electric vector. This is averaged in a powdered sample.

Hydrothermal beryl grown in the absence of alkalis shows only the type-I absorption band (Wood and Nassau 1967; Schmetzer 1989). It was concluded that H_2O molecules adjacent to alkali metal ions are able to rotate from the perpendicular to the parallel position by the effect of the electric field of the charged alkali cation. Alkali is coordinated on both sides by two type-II H_2O molecules (Goldman et al. 1978). Type-II H_2O and total (Na + K + Ca) show a characteristic 2/1 ratio in cordierite (Vry et al. 1990); a rough 2/1 relation between total H_2O and alkalis was also recognized by Sherriff et al. (1991) in beryl. Computed type-II H_2O content (Table 3) far exceeds that predicted by this ratio. Schmetzer (1989) reported a statistical approach using infrared absorption spectra from 103 natural and synthetic emerald specimens with a wide range of alkali (Na, Li, or both) content. The three classical stretching vibrational bands of Wood and Nassau (1968) were generally expressed as follows: band A = 3694 cm^{-1}, band B = 3592 cm^{-1}, band C = 3655 cm^{-1} (see Table 2 for their assignments). Schmetzer (1989) assumed a positive correlation between alkali content and the peak intensity of bands B and C, which correspond to molecules of type-II H_2O that were supposed to be bonded to adjacent alkali ions in the channel. Type-IIa H_2O would correspond to the sequence H_2O-Na-H_2O, and type-IIb H_2O to the sequence H_2O-Na-□ (OH group is unlikely). Beryl from Serra Branca shows A > B ≫ C in the band-intensity distribution (Fig. 3), which corresponds to an alkali-poor beryl of group II (Schmetzer 1989) with Na_2O content in the range 0.03–0.5 wt%. Above considerations suggest that even type-IIb H_2O is minor and that a large percentage of the (C2) sites in the channel would remain vacant.

Micro Raman spectroscopy. Very little characterization has been performed on beryl using Raman spectroscopy. Narayanan (1950) provided a low-frequency spectrum of beryl with little detail. More recent Raman studies, mostly in conjunction with IR-reflectance experiments, have confirmed the occurrence of the major active modes of vibration predicted by factor-group analysis (Gervais and Piriou 1972; Adams and Gardner 1974; Hofmeister et al. 1987). Micro Raman scattering spectra (Fig. 4) were recorded at room temperature on the same wafers used in the IR investigation, using a multichannel (1024 diodes) DILOR XY microspectrometer equipped with a Spectra Physics argon ion laser (514.5 nm exciting line, 1 W laser power; J. Dubessy operator, CREGU, Nancy). Experiments were conducted with different orientations of the electric vector, **E**, with regard to the *c* axis of beryl. Spectra were acquired over the characteristic Raman frequencies of H_2O and CO_2, with a resolution of approximately 2 cm^{-1}. Whatever the crystallographic orientation (normal or parallel to the *c* axis), the H_2O signal is similar in intensity and position (3606 and 3597 cm^{-1} as a shoulder), suggesting at least two orientations in roughly equal

TABLE 3. Respective contents of type-I and type-II H_2O and molar absorptivity coefficients ϵ from powder and in situ experiments

	KBr pellet				In situ			
	A.U.	wt%	Moles pfu	Apparent ϵ	A.U.	wt%	Moles pfu	Real ϵ
H_2O type I (3698 cm^{-1})	0.062	0.99	0.307	50	1.63	1.09	0.338	197
H_2O type II (3653 cm^{-1})	0.058	0.92	0.285	50	1.22	0.82	0.254	197
CO_2 (2361 cm^{-1})	0.022	0.19	0.024	225	1.13	0.19	0.024	322

Note: Beer's law is expressed as $A = \epsilon bC$, with A = the measured absorbance (in absorbance units, A.U.), ϵ = an absorptivity coefficient (in liters per mole-centimeter), b = the path length, i.e., sample thickness (in centimeters), and C = the concentration (in moles per liter).

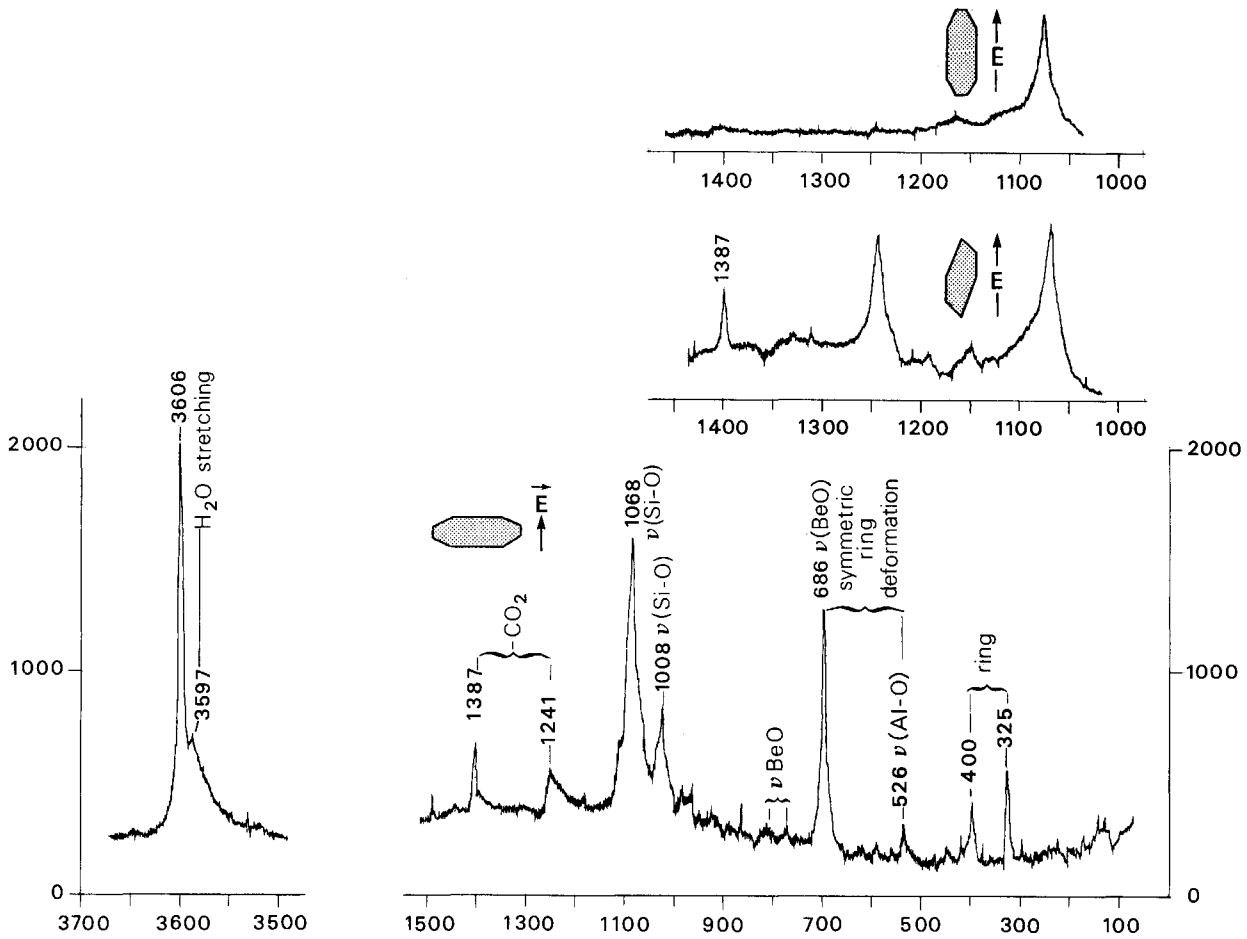

FIGURE 4. Raman-scattering spectra of beryl (*c* axis horizontal); inset: expression of the CO_2 peaks in relation to the orientation of the beryl section.

proportions for the H_2O molecules. CO_2 is represented by two complementary peaks at 1387 cm^{-1} ($2\nu_2$) and 1241 cm^{-1} (ν_1), corresponding to the Fermi doublet. A portion (1450–1000 cm^{-1}) of the spectrum range presented as insets in Figure 4 shows the complete disappearance of the CO_2 bands when **E** is parallel to the *c* axis, which indicates that the CO_2 molecule is oriented normally to the channel axis. There is also a reversal in intensity with **E** orientation between peaks at 1387 and 1241 cm^{-1}, although the reason for this is not understood. All peaks between 1100 and 300 cm^{-1} result from Si-O (symmetric ring deformation in the range 700–500 cm^{-1} and satellites at 400 and 325 cm^{-1}), Be-O, and Al-O bonding [assignments according to Adams and Gardner (1974)].

NMR spectroscopy

Along with IR absorption spectroscopy, proton nuclear magnetic resonance (NMR) spectroscopy is a promising technique for the investigation of the structural environment of O-bound H species (H_2O molecules and OH groups) in minerals, especially nonstoichiometric H. However, very appropriate and restrictive experimental conditions (field strength, spinning speed, etc.) are required to characterize the form, site, motion, and environment of H in a mineral structure.

The ^1H MAS (magic-angle-spinning) NMR experiment on powdered beryl was performed at room temperature at 300 MHz with a Bruker MSL-300 multinuclear Fourier-transform spectrometer housed at the Nancy I University (Lab. Méthodologie RMN). The external magnetic field was 7 Tesla (300.13 MHz). The beryl sample (50 μm in grain size) was spun at 4.6 kHz. The spectrum (Fig. 5) is the average of 332 scans with a recycle delay of 5 s per scan. The high resolution obtained in the spectrum exhibits a very distinctive spinning-sideband pattern. Even if some asymmetrical geometry is observed, the pattern clearly has the spectral appearance expected for a Pake doublet, a behavior that is symptomatic of the inhomogeneous character of the dipolar interaction in isolated homonuclear two-spin systems (i.e., structurally isolated

H_2O molecules; Yesinowski et al. 1988). Similar doublet lines were already found in static (non-MAS) ^1H NMR experiments on oriented single crystals of beryl (Paré and Ducros 1964) and cordierite (Tsang and Ghose 1972; Carson et al. 1982). The overall width of the beryl spectrum would indicate the absence of significant communication between clusters of spin pairs, which would have limited relative mobility (i.e., diffusion by translation) along the channels. However, spinning-sideband peaks in Figure 5 are very broad. There are several reasons for this broadening: (1) Possible H clustering (homogeneous broadening) inside the channel, as cited by Vry et al. (1990) for cordierite. (2) Possible intermolecular dipolar interactions with neighboring H_2O molecules, with unpaired electron spins localized on paramagnetic metal ions (Fe in our case), or short-range proton-Al or -Na dipolar couplings. These interactions create a heterogeneous distribution of proton resonance lines, which in combination increase line width (chemical-shift or heterogeneous broadening), as described by Carson et al. (1982) in cordierite. (3) Occurrence of H in chemically distinct OH sites such as those in mica inclusions. A ^1H MAS NMR spectrum of phengite from the host rock (Fig. 5) was obtained with the same experimental conditions used for beryl. It shows only one broad resonance peak as a homogeneous enlargement of the spectrum (full width at half height of 20 kHz) without any discernable lateral spinning sidebands. The disturbing influence of paramagnetic cations can also be invoked. This broad experimental line shape can be fitted well with a Gaussian function, which suggests that there is only one proton next-nearest-neighbor environment within the phengite structure (Cho and Rossman 1993). From the above considerations, one can affirm that phengite partly contributes to the broad size of the centerband and the first and second sideband lines shown in the beryl spectrum.

The results of different spectroscopic studies have sparked an important controversy in the literature about the orientation and motion of the H_2O molecules with regard to the channel axis. The NMR measurements of Carson et al. (1982) on cordierite, in contrast to those of an IR investigation on the same sample (Goldman et al. 1977), indicate that at room temperature there is only one kind of dynamically distorted H_2O molecule undergoing anisotropic reorientational motion, i.e., jumping back and forth between two perpendicular orientations (the two-site hopping model), in a time scale that is short in comparison with the NMR line width (about 10^{-5} s at room temperature) but long in comparison with the IR vibrational frequency (about 10^{-12} s). The greatest residence time of the H-H vector would be parallel to the channel axis (type-I H_2O). Because of the long time scale for NMR measurements, this technique can be used to observe only a long-term average. On the basis of quasi-elastic neutron scattering experiments conducted on powdered cordierite, Winkler et al. (1994) proposed the alternative model of one rigid molecule revolving around its center of gravity but maintaining the permanent orientation of its H-H vector parallel to the *c* axis. However, the clear definition of two perpendicular orientations for H_2O in the infrared experiments (Fig. 2a) is inconsistent with a fixed orientation of the proton-proton vector. The data set obtained in the present study, though, is too limited for more definite conclusions.

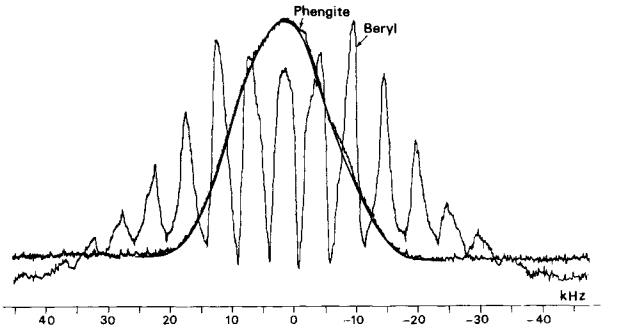

FIGURE 5. The ^1H MAS NMR spectra of beryl and phengite at 300 MHz.

MASS SPECTROMETRY AND ANALYSIS OF VOLATILES

To determine the amount of volatiles, our mass spectrometry studies included thermal analysis. Volatiles from beryl and phengite were extracted by pyrolysis under vacuum in a quartz furnace at temperatures up to 1000 °C. The heating rate was monitored according to the ambient pressure above the sample, i.e., by the devolatilization rate. Mass spectra of volatiles were recorded with a Balzers Quadstar 420 mass spectrometer (G. Gerard operator, LEM-ENSG Nancy). One hundred twenty milligrams of beryl and 130 mg of phengite (grain size of 25 μm) were used. Weight loss after heating was 2.13% for beryl and 4.59% for phengite. Degassing profiles (ionization current vs. temperature) for relative masses 2, 12, 18, 20, 40, and 44 are shown in Figure 6. The low-temperature spectrum is insignificant and must correspond to degassing of the adsorbed moisture on the finely ground samples. Structural damage began at 550 °C, and both beryl and phengite dehydrated over a fairly wide temperature range: from 550 to 850 °C for beryl, whereas phengite had not yet dehydrated at 1000 °C. CO_2 from beryl was lost at the significantly higher temperature of 850 °C. A similar temperature range was found for dehydration and decarbonation reactions in cordierite and beryl through the broadening and then vanishing of the H_2O bands of vibration between 800 and 1000 °C (Aines and Rossman 1984; Polupanova et al. 1985; Giampaolo and Putnis 1989), whereas Brown and Mills (1986) found little dehydration (little effect on the occupancies of the channel sites) of a beryl from pegmatite after heating to 800 °C.

The degassing curves for H_2 (mass 2) and CO (mass 28) are close to those of H_2O and CO_2, respectively. Because concentrations of CO and H_2 are negligible below 600 °C under normal conditions of equilibrium in the Earth's crust (Dubessy 1984), it is likely that both species were

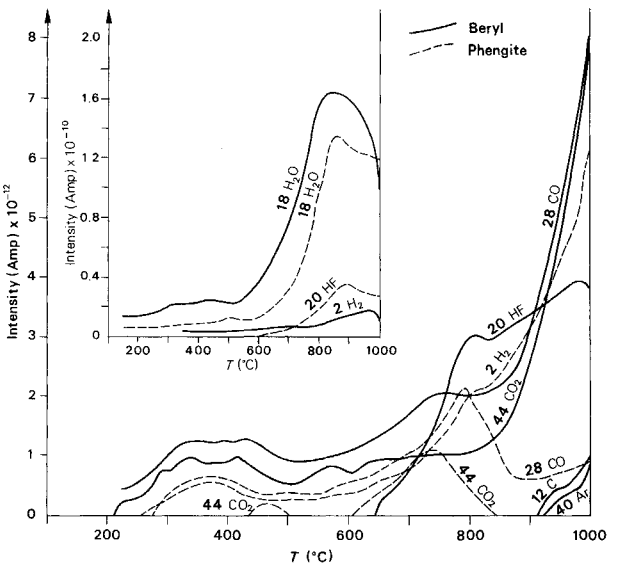

FIGURE 6. Degassing profiles (ionization current vs. temperature) for relative masses 2, 12, 18, 20, 40, and 44 from mass spectrometry experiments on beryl and phengite.

produced by reduction of H_2O and CO_2 during the course of the heating experiments. Even reduction up to C genesis (mass 12) is possible at 900 °C for beryl. HF (mass 20) is significant only in mica.

In our case, the plugging effect of alkalis cannot explain why the release of volatiles from the channels requires such high temperatures.

DISCUSSION

Measured vibrational spectra of single crystals confirm the occurrence of two types of molecular H_2O with perpendicular orientations in beryl channels. Their ν_3 absorbance intensities, converted to their respective amounts, show slightly more type-I orientation than type-II. Solid-state proton NMR results suggest, at least at the time scale of the NMR line width, that H_2O molecules have only relatively limited mobility between these two perpendicular orientations. The ratio of type-II H_2O to alkalis generally exceeds two, in disagreement with data from the literature obtained mainly on beryl from pegmatites. Vibrational frequencies of H_2O and CO_2 obtained during this investigation are close to those of vapor phases, suggesting that molecules are loosely bonded to O atoms of the silicate framework. CO_2 is definitely perpendicular to the channels of beryl without any preferential orientation inside the (0001) plane. The high temperatures necessary for devolatilization suggest that the channels of beryl are relatively closed, in apparent contrast with those of cordierite. If fluid inclusion microthermometry were unable to shed light on the physical conditions prevailing during the growth of these beryl phenocrysts, their volatile characteristics would confirm the strongly hydrated and alkali-depleted nature of the growth medium, in contrast with the alkali-dominated medium encountered during pegmatite genesis.

ACKNOWLEDGMENTS

The authors thank P. Tekely for assistance and helpful discussions concerning the NMR investigation. The helpful comments on an earlier version of the manuscript by two anonymous reviewers are much appreciated. The authors are indebted to L. Reisberg for extensive improvement of the English text, and to Y. Lestreit for illustrations. This paper is contribution no. 1157 of the Centre de Recherches Pétrographiques et Géochimiques.

REFERENCES CITED

Adams, D.M., and Gardner, I.R. (1974) Single-crystal vibrational spectra of beryl and dioptase. Journal of the Chemical Society, Dalton Transactions, 1502–1506.

Aines, R.D., and Rossman, G.R. (1984) The high temperature behavior of water and carbon dioxide in cordierite and beryl. American Mineralogist, 69, 319–327.

Armbruster, T. (1986) Role of Na in the structure of low-cordierite: A single-crystal X-ray study. American Mineralogist, 71, 746–757.

Artioli, G., Rinaldi, R., Ståhl, K., and Zanazzi, P.F. (1993) Structure refinements of beryl by single-crystal neutron and X-ray diffraction. American Mineralogist, 78, 762–768.

Aurisicchio, C., Fioravanti, G., Grubessi, O., and Zanazzi, P.F. (1988) Reappraisal of the crystal chemistry of beryl. American Mineralogist, 73, 826–837.

Aurisicchio, C., Grubessi, O., and Zecchini, P. (1994) Infrared spectroscopy and crystal chemistry of the beryl group. Canadian Mineralogist, 32, 55–68.

Bakakin, V.V., and Belov, N.V. (1962) Crystal chemistry of beryl. Geochemistry, 5, 484–500.

Barton, M.D. (1986) Phase equilibria and thermodynamic properties of minerals in the BeO-Al_2O_3-SiO_2-H_2O (BASH) system, with petrologic applications. American Mineralogist, 71, 277–300.

Boutin, H.G., Safford, G.J., and Danner, H.R. (1964) Low-frequency motions of H_2O molecules in crystals. Journal of Chemical Physics, 42, 1469–1470.

Brown, G.E., Jr., and Mills, B.A. (1986) High-temperature structure and crystal chemistry of hydrous alkali-rich beryl from the Harding pegmatite, Taos County, New Mexico. American Mineralogist, 71, 547–556.

Carson, D.G., Rossman, G.R., and Vaughan, R.W. (1982) Orientation and motion of water molecules in cordierite: A proton nuclear magnetic resonance study. Physics and Chemistry of Minerals, 8, 14–19.

Černý, P., and Turnock, A.C. (1975) Beryl from the granitic pegmatites at Green Lake, Southeastern Manitoba. Canadian Mineralogist, 13, 55–61.

Charoy, B., and Noronha, F. (1996) Multistage growth of a rare-element, volatile-rich microgranite at Argemela (Portugal). Journal of Petrology, 37, in press.

Cho, H., and Rossman, G.R. (1993) Single-crystal NMR studies of low-concentration hydrous species in minerals: Grossular garnet. American Mineralogist, 78, 1149–1164.

Damon, P.E., and Kulp, J.L. (1958) Excess helium and argon in beryl and other minerals. American Mineralogist, 43, 433–459.

de Almeida Sampaio Filho, H., and Sighinolfi, G.P. (1973) Contribution to the crystal chemistry of beryl. Contributions to Mineralogy and Petrology, 38, 279–290.

de Andrade, G.F. (1978) As mineralizações de estanho, berílio e cobre do Granito Serra Branca, Cavalcante-GO. Tese, Universidade de Brasília, Brazil.

Dubessy, J. (1984) Simulation des équilibres chimiques dans le système C-O-H: Conséquences méthodologiques pour les inclusions fluides. Bulletin de Minéralogie, 102, 600–610.

Duyckaerts, G. (1959) The infrared analysis of solid substances. Analyst, 84, 201–204.

Franks, F. (1972) The properties of ice. In F. Franks, Ed., Water: A com-

prehensive treatise, volume 1: The physics and physical chemistry of water, p. 115–149. Plenum, New York.

Gervais, F., and Piriou, B. (1972) Etude des spectres de réflexion infrarouge du béryl dans la région 280–400 cm^{-1}. Comptes Rendus de l'Académie des Sciences de Paris, 274, 252–255.

Giampaolo, C., and Putnis, A. (1989) The kinetics of dehydration and order-disorder of molecular H_2O in Mg-cordierite. European Journal of Mineralogy, 1, 193–202.

Gibbs, G.V., Breck, D.W., and Meagher, E.P. (1968) Structural refinements of hydrous and anhydrous synthetic beryl, $Al_2(Be_3Si_6)O_{18}$ and emerald $Al_{1.9}Cr_{0.1}(Be_3Si_6)O_{18}$. Lithos, 1, 275–285.

Goldman, D.S., Rossman, G.R., and Dollase, W.A. (1977) Channel constituents in cordierite. American Mineralogist, 62, 1144–1157.

Goldman, D.S., Rossman, G.R., and Parkin, K.M. (1978) Channel constituents in beryl. Physics and Chemistry of Minerals, 3, 225–235.

Hofmeister, A.M., Hoering, T.C., and Virco, D. (1987) Vibrational spectroscopy of beryllium aluminosilicates: Heat capacity calculation from band assignments. Physics and Chemistry of Minerals, 14, 205–224.

Johannes, W., and Schreyer, W. (1981) Experimental introduction of CO_2 and H_2O into Mg-cordierite. American Journal of Science, 281, 299–317.

Lamb, W.M. (1985) C-O-H fluid calculations and granulite genesis. In A.C. Tobi and J.L.R. Touret, Eds., The deep Proterozoic crust in the North Atlantic Province, p 119–131. Reidel, Dordrecht, the Netherlands.

Le Breton, N. (1989) Infrared investigation of CO_2-bearing cordierites: Some implications for the study of metapelitic granulites. Contributions to Mineralogy and Petrology, 103, 387–396.

Nakamoto, K. (1963) Infrared spectra of inorganic and coordination compounds, 328 p. Wiley, New York.

Narayanan, P.S. (1950) The Raman spectrum of beryllium silicate. Proceedings of the Indian Academy of Sciences, Bangalore, 31A, 354–358.

Paré, X., and Ducros, P. (1964) Etude par résonance magnétique nucléaire de l'eau dans le béryl. Bulletin de la Société française de Minéralogie et de Cristallographie, 87, 429–433.

Pedersen, B. (1964) NMR in hydrate crystals: Correction for vibrational motion. Journal of Chemical Physics, 41/1, 122–132.

Polupanova, T.I., Petrov, V.L., Kruzhalov, A.V., Laskovenkov, A.F., and Nikitin, V.S. (1985) The thermal stability of beryl. Geochemistry International, 22, 11–13.

Pouchou, J.L., and Pichoir, F. (1991) Quantitative analysis of homogeneous or stratified microvolumes applying the model "PAP." In K.F.J. Heinrich and D.E. Newbury, Eds., Electron probe quantitation, p. 31–75. Plenum, New York.

Schmetzer, K. (1989) Types of water in natural and synthetic emerald. Neues Jahrbuch für Mineralogie Monatshefte, 1, 15–26.

Sherriff, B.L., Grundy, D.H., Hartman, J.S, Hawthorne, F.C., and Černý, P. (1991) The incorporation of alkalis in beryl: Multi-nuclear MAS-NMR and crystal structure study. Canadian Mineralogist, 29, 271–285.

Staatz, M.H., Griffitts, W.R., and Barnett, P.R. (1965) Differences in the minor element composition of beryl in various environments. American Mineralogist, 50, 1783–1795.

Tsang, T., and Ghose, S. (1972) Nuclear magnetic resonance of ^1H and ^{27}Al and Al-Si order in low cordierite, $Mg_2Al_4Si_5O_{18} \cdot nH_2O$. Journal of Chemical Physics, 56/7, 3329–3332.

Visser, D., Kloprogge, J.T., and Maijer, C. (1994) An infrared spectroscopic (IR) and light element (Li, Be, Na) study of cordierites from the Bamble Sector, South Norway. Lithos, 32, 95–107.

Vry, J.K., Brown, P.E., and Valley, J.W. (1990) Cordierite volatile content and the role of CO_2 in high-grade metamorphism. American Mineralogist, 75, 71–88.

Wickersheim, K.A., and Buchanan, R.A. (1959) The near infrared spectrum of beryl. American Mineralogist, 44, 440–445.

Winkler, B., Coddens, G., and Hennion, B. (1994) Movement of channel H_2O in cordierite observed with quasi-elastic neutron scattering. American Mineralogist, 79, 801–808.

Wood, D.L., and Nassau, K. (1967) Infrared spectra of foreign molecules in beryl. Journal of Chemical Physics, 47, 2220–2228.

——— (1968) The characterization of beryl and emerald by visible and infrared absorption spectroscopy. American Mineralogist, 53, 777–800.

Yesinowski, J.P., Eckert, H., and Rossman, G.R. (1988) Characterization of hydrous species in minerals by high-speed ^1H MAS-NMR. Journal of the American Chemical Society, 110, 1367–1375.

Zimmermann, J.L. (1981) La libération de l'eau, du gaz carbonique et des hydrocarbures des cordiérites: Cinétique des mécanismes: Détermination des sites: Intérêt pétrogénétique. Bulletin de Minéralogie, 104, 325–338.

Manuscript received March 24, 1995
Manuscript accepted November 14, 1995